Polym. Bull. (2012) 68:493–505
DOI 10.1007/s00289-011-0644-3

ORIGINAL PAPER

Investigating the UV-curing performance for polyacrylated polymer in dendritic and regular conformation

Syang-Peng Rwei · Jung-Da Chen

Received: 3 July 2011 / Revised: 22 September 2011 / Accepted: 24 September 2011 /

Abstract In this study, PDSC was employed to monitor the UV curing process for dendritic and regular monomers with various acrylate sites. Experimental results reveal that even with only a small increase in molecular weight for regular monomers caused a large increase in viscosity. A dendritic monomer with the same number of sites has a much lower viscosity. The conversion of hydroxyl groups into acrylic groups in the dendritic monomer slightly reduces the viscosity by destroying the hydrogen bonds. The curing conversion and curing rate increased with the number of acrylate sites to maxima at five. The acceleration of the double bond reaction within a dense group of multiacrylate sites is responsible for the initial rise, but the steric effect of the branches, hindering the simultaneous free-radical propagation, causes a decline as the number of sites increases in the curing of dendrimers. The autocatalyzed reaction model was then applied to simulate the curing results from PDSC. Dendrimers with 10–19 acrylate sites were found to have lower rate constant k and smaller autocatalyzed order *m* than the traditional ones. Finally, the heterogeneity of the cross-linking density of dendrimers generally causes dendritic monomers to have weaker hardness and lower T_d values than the regular ones. Nevertheless, dendrimers with 19 acrylate sites yield a film having low processing viscosity, satisfactory hardness (6H), reasonable T_d (290 °C), and a superior refractive index (1.5).

Keywords UV curing · Photo-DSC · Regular monomer · Dendrimer · Acrylate site

---

S.-P. Rwei (✉) · J.-D. Chen
Institute of Organic and Polymeric Materials, National Taipei University of Technology,
#1, Sec 3, Chung-Hsiao E. Rd., Taipei, Taiwan, ROC
e-mail: f10714@ntut.edu.tw

Introduction

UV curing technology has spread rapidly throughout many industrial sectors and is used to produce protective coatings, wire insulation, adhesives, and electronic packaging [1–4]. It has many economic advantages over the usual thermal curing process because it is high-speed and consumes little energy, involves room-temperature treatment, is highly efficient, and does not involve the use of solvents. The need for extremely short curing times, commonly under 1 s, in such areas as ink-jet printing and optical-fiber coating has made UV curing a uniquely effective technology.

A typical UV curing process begins with a mixture of liquid materials that comprise initiators and multifunctional oligomers and monomers. The reactive liquid-mixture is then exposed to UV light to convert multifunctional oligomers and monomers into solid-like crosslinked networks by the cleavage of bonds between the unsaturated groups. Chemists have recently examined various approaches to monitor UV curing, including the real-time infrared (FTIR) method [5, 6], Raman spectroscopy [7], fluorescence spectroscopy [8], photoacoustic spectroscopy [9, 10], rheological analysis [11], and photo-differential scanning calorimetry (PDSC) [12–15]. Of these, PDSC has been the most successful and is extensively utilized in many rapid curing systems. PDSC is basically a modified DSC, with an Hg lamp source mounted next to the sample. The following section presents a description of PDSC characterization principle in detail.

Dendrimer, from the Greek word (dendron) for tree, refers to macromolecules with branching reach out from central core. This structural characteristic enables dendrimers to have a high degree of molecular uniformity, a narrow molecular weight (MW) distribution, specific size and shape characteristics, and highly functionalized end groups at their globular periphery. In late 1970s, Donald Tomalia, a Dow researcher, began to build the first of these branching molecules. Since then, many new dendrimers have been developed and tuned for particular applications [16–20] such as drug delivery, catalysts, and optoelectronic usage. One potential use is in coatings used as viscosity mediators during curing. In solution, linear chains are present as flexible coils, while dendrimers are present tightly packed balls. These formations have a strong effect on their rheological properties. Dendrimer solutions have significantly lower viscosity than regular polymers [21]. Rapid curing of a regular monomer depends on the presence of multifunction branches in a molecule, which increase the molecular mass, the complexity of molecular structure, and dramatically the intrinsic viscosity. Balancing the viscosity with the cure speed using a conventional monomer is very difficult. A dendrimer, however, can be used in a new coating formula with a highly UV-reactive structure but low viscosity, to accelerate curing and improve some of the optical properties of the coated film. Although remarkable progress has been made in the applications of dendrimers in various fields as mentioned above, studies of the use of dendrimers in the UV curing process are lacking. In this study, PDSC was adopted to monitor UV curing of dendrimers and regular monomers with various reactive groups. The results in this study can be applied to evaluate the ideal formulation of some UV curing reactions, specifically their meeting the requirement of a short reaction period.

Experimental

Curing reagents

Boltorn P500 (Perstorp, Sweden), a third-generation dendrimer with 19 branches of hydroxyl groups (Scheme 1) and a average MW of 1932 (Fig. 1), was applied as a virgin dendrimer. Various amounts of acrylic acid (34.02, 45.36, 56.7, 113.4, and 215.46 g, Acros) were reacted with Boltorn P500 (300 g per case) to prepare UV-curable dendrimers with 3, 4, 5, 10, and 19 acrylate sites per molecule, denoted DM-3, DM-4, DM-5, DM-10, and DM-19, respectively. Toluene was used as the solvent to obtain a solution with a solid content of 50.5%. A small amount (approximately 0.5 wt%) of *p*-toluene sulfonic acid (PTSA, Acros) and a tiny amount of phenothiazine (0.4 g, Acros) were employed as the catalyst and the inhibitor, respectively. The reactions were initially performed at 70 °C for 30 min with stirring to dissolve the dendrimer into the solution. The esterification reaction was then conducted at 105 °C for various periods to yield different acrylate sites. The synthesized product was purified by washing repeatedly in toluene. The water condensed by the esterification reaction (Scheme 2) was collected in a side reflux beaker.

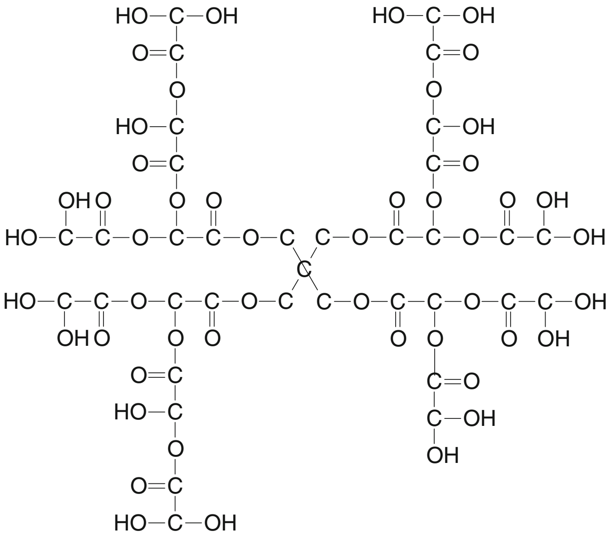

Scheme 1 Structure of Boltorn P500 (Perstorp, Sweden), a third-generation dendrimer with 19 branches of hydroxyl groups

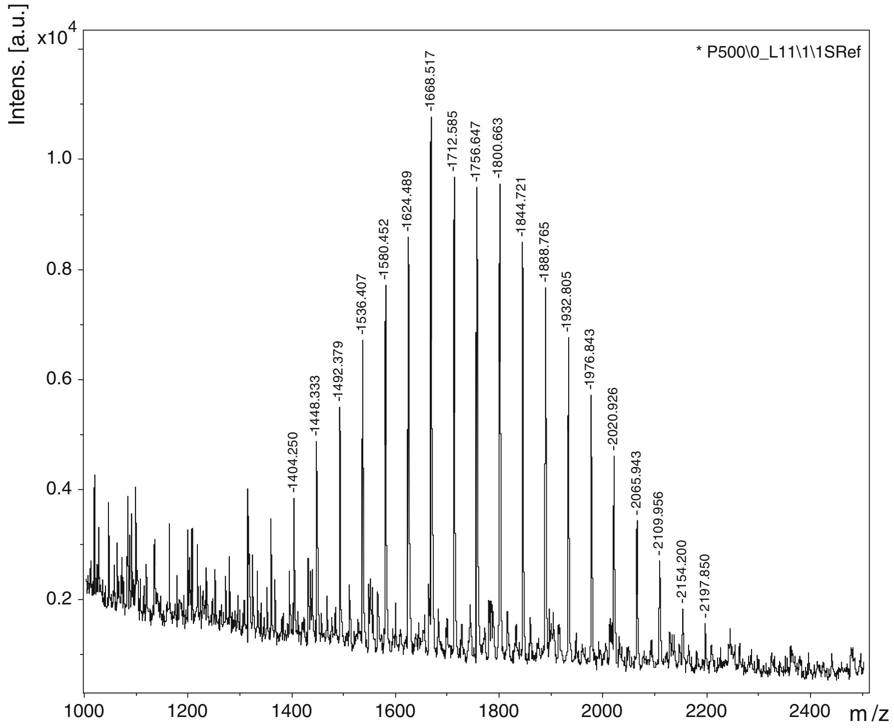

Fig. 1 Maldi/Tof spectrum of Boltorn P500's (MW: 1932 g/mol)

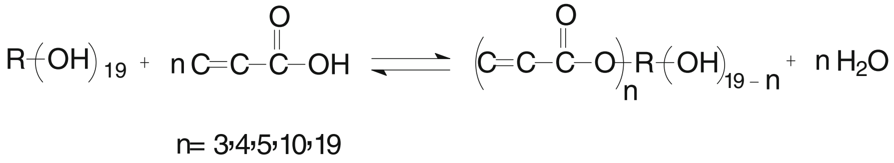

$$R\left(OH\right)_{19} + n\,C{=}C{-}\overset{\overset{O}{\|}}{C}{-}OH \rightleftharpoons \left(C{=}C{-}\overset{\overset{O}{\|}}{C}{-}O\right)_{n}R\left(OH\right)_{19-n} + n\,H_2O$$

$n = 3, 4, 5, 10, 19$

Scheme 2 The preparation of acrylated dendrimer by the esterification reaction

The number of acrylate sites was first determined by the IR detection, and then was confirmed from the amount of condensed water (Table 1). Notably, small amount of acrylic acid would come out with condensed water due to the azeotropic situation, and the amount of actual dehydration shown in Table 1 is thus slightly greater than the theoretical value. Moreover, number of acrylate sites can be reconfirmed by titration analysis thereafter. 0.1 N of KOH along with phenolphthalein as an indicator were employed in the titration process. Four regular monomers applied in this UV curing study (Scheme 3), HDDA (1,6-Hexanediol diacrylate), TMPTA (trimethylolpropane triacrylate), PETA (pentaerythritol tetraacrylate), and DPHA (dipentaerythritol hexaacrylate) with 2, 3, 4, and 6 reaction sites, respectively, denoted as L-2, L-3, L-4, and L-6, were kindly provided by Double Bond Chemical Co. (Taiwan, R.O.C.).

Table 1 The results of dehydration and FTIR comparison for the esterification reaction of Boltorn P500

	DM-3	DM-4	DM-5	DM-10	DM-19
Dehydration					
Theoretical amount of dehydration (mL)	8.1	10.8	13.5	27	51.3
The amount of actual dehydration (mL)	9.7	12.9	16.2	32.4	61.5
FTIR comparison					
Vinyl group peak 810 cm^{-1} (T%)	84.11	76.97	73.52	67.03	57.27
Carbonyl group peak 1726 cm^{-1} (T%)	78.68	72.62	68.35	54.15	35.41

Name	Structure	MW
1,6 Hexanediol diacrylate(L2)	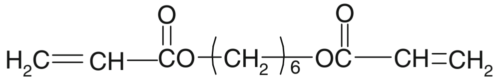 $H_2C{=}CH{-}\overset{O}{\overset{\|}{C}}O{\left(CH_2\right)}_6O\overset{O}{\overset{\|}{C}}{-}CH{=}CH_2$	224.25
Trimethylolpropane triacrylate(L3)	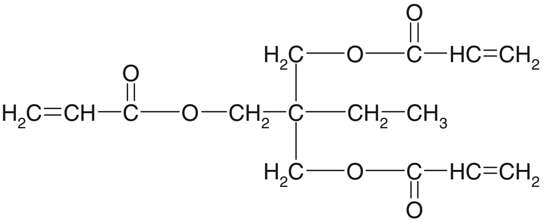	296.32
Pentaerythritol tetraacrylate(L4)	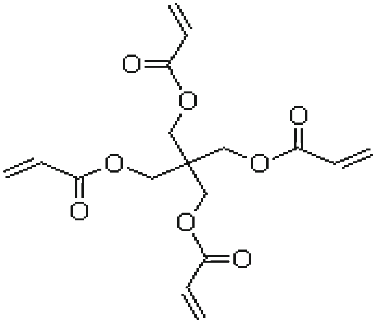	352.34
Dipentaerythritol hexaacrylate(L6)	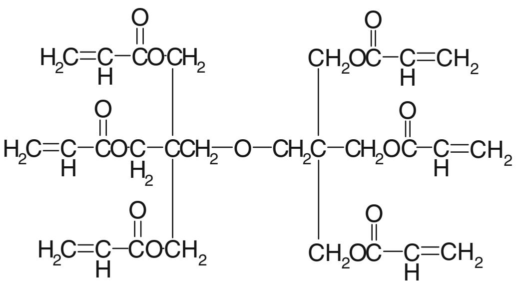	578.56

Scheme 3 Structure of L-2, L-3, L-4, and L-6 (DBC, Taiwan)

A fix amount, 3 wt%, of the photoinitiator, 2-hydroxy-2-methylpropiophenone (Darocur 1173, CAS 7473-98-5, Double Bond Chemical Co.) was used and well blended with the regular or dendritic monomers in a solvent-free condition. About 10 mg of the prepared sample per test was applied for examing the UV curing study by PDSC at 35 °C. All the chemicals were reagent-grades and were used without further purification. The refractive index values of liquid oligomers were measured with an Abbe′ refractometer. And this measurement in this study was performed at 25 °C.

Characterization

The curing reaction was monitored using a Perkin-Elmer DPA 7 (Double Beam Photocalometric Assessory)—a PDSC design based on two identical UV beams and joined to a Perkin's DSC 7 system. Wavelengths between 250 and 600 nm are used. The intensity of a UV lamp is 2 W/cm^2, and source varies with age and other variables, so the DPA 7 includes a photofeedback control loop to maintain constant lamp intensity. During the UV curing experiment, any thermal flow into and out of the sample is instantaneously detected because the small mass of the furnaces is low (less than 10 mg) and the platinum resistance detector responds immediately. This rapid response is critical when some photocuring reaction is completed in only a few seconds after exposure to UV light. The DSC thermograms are recorded simultaneously during exposure, and both the reaction rate and the degree of polymerization can be calculated. After baseline correction, both the polymerization rate and the reaction conversion were determined according to Eqs. 1 and 2, respectively [22].

$$R_{\mathrm{p}}=[\triangle H_{\mathrm{t}}/t]/[n_0\triangle H_0 W_0/M_0] \tag{1}$$

$$\alpha=\int R_{\mathrm{p}}\mathrm{d}t \tag{2}$$

where R_{p} is the reaction rate; $\Delta H_t/t$ is the heat flow per second during reaction; n_0 is the number of double bond per monomer; M_0 is the molar mass of the monomer; ΔH_0 is the heat generated per mole of double bond of the monomer; W_0 is the mass of monomer in the sample; and α is corresponding the reaction conversion ratio. Notably, the reaction heat, ΔH_0, used herein was 20.6 kcal/mol for the acrylate double bond [23].

Infrared spectra were obtained using a Jasco FT/IR-480. Thermogravimetric analytic (TGA) thermograms were obtained using a Perkin-Elmer TGA-7 in a dry nitrogen atmosphere at the set heating rate. The shear viscosity measurements for the polyacrylate samples before UV exposure were made using a Rheometric SR-5 rheometer. The hardness test applies ASTM D3363-05 standard method for film hardness by "pencil test".

The refractive index *n* of the cured samples was measured by a refractometer (DR-A1, Atago, Japan). The MW for all the regular monomers was provided by the supporter (Double Bond Chemical Co). The MW of the dendrimers, however, was obtained by the Maldi/Tof–Tof Mass Spectrometer (Bruker Autoflex III TOF/TOF). A typical Maldi/Tof Mass Spectrum for the Boltorn P500 was shown in Fig. 1. The average number of the MW distribution curve is 1932 g/mol, close to the theoretical MW of Boltorn P500. The MW of acrylated samples modified from Boltorn P500 was also characterized by the Maldi/Tof–Tof Mass Spectrometer to double confirm the number of acrylated sites connected to the dendrimers.

Results and discussion

Figure 2 shows the IR spectra for Boltorn P500 with various numbers of acrylated sites. The acrylate double bonds can be monitored by appearance of the peak intensity of absorption band around 810 cm^{-1}. Carbonyl peak at 1723 cm^{-1} was used as a calibration standard. The stoichiometry of the acrylate sites in Boltorn P500 and peak intensity of double bonds at 810 cm^{-1} reveal a similar trend. Table 1 presents the results of acrylate site number analyzed by the condensed water from esterification. The theoretical value and the experimental result also showed a good match, reconfirming the good control of dehydration of Boltorn P500 to obtain various numbers of acrylated branches.

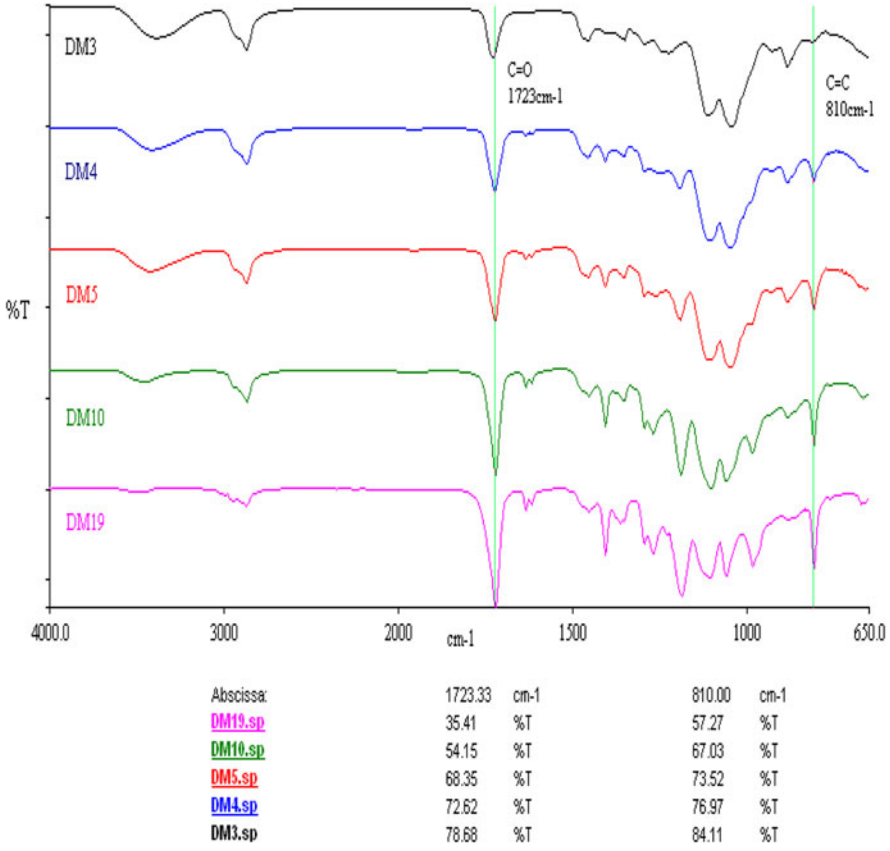

Abscissa:	1723.33	cm-1	810.00	cm-1
DM19.sp	35.41	%T	57.27	%T
DM10.sp	54.15	%T	67.03	%T
DM5.sp	68.35	%T	73.52	%T
DM4.sp	72.62	%T	76.97	%T
DM3.sp	78.68	%T	84.11	%T

Fig. 2 FTIR spectra of the product dendrimer monomers and Boltorn P500

Figure 3 presents the effect of the MW on the viscosity of traditional and dendritic monomers. The MW of regular monomers increase remarkably when it has more branches attached to the main chain; however, the dendrimer Boltorn P500 with fixed number of branches, 19, has a slight MW rises because of the conversion of the hydroxyl groups into acrylic groups. Figure 3 displays a significant increase in viscosity with the number of branches of the regular monomers, even given a slight increase in MW. The viscosity trace (dotted line in Fig. 3) indicates that the viscosity of the regular monomers increases by a 1.5 orders of magnitude as the number of branches rises to 19. A comparison with the regular monomers demonstrates that a dendritic monomer containing with the same number of branches, 19, has a much lower viscosity. This implies a great advantage for applying dendritic monomers in a precise coating area in the future. Finally, Fig. 3 shows that the conversion of hydroxyl groups into acrylic groups for the dendritic-type monomer slightly reduces the viscosity because the hydrogen bonds are eliminated.

Figure 4 plots the curing conversion versus time, for both regular and dendritic monomers that contain various numbers of acrylic sites, to demonstrate the effect of the dendritic structure on the conversion. Figure 4 reveals three interesting results. First, the dendritic monomer (DM-4) has almost double the conversion ratio of the regular monomer (L-4) with the same number of acrylic groups. Second, of the regular monomers, L-6 has the highest final conversion, followed by L-4, L-3, and

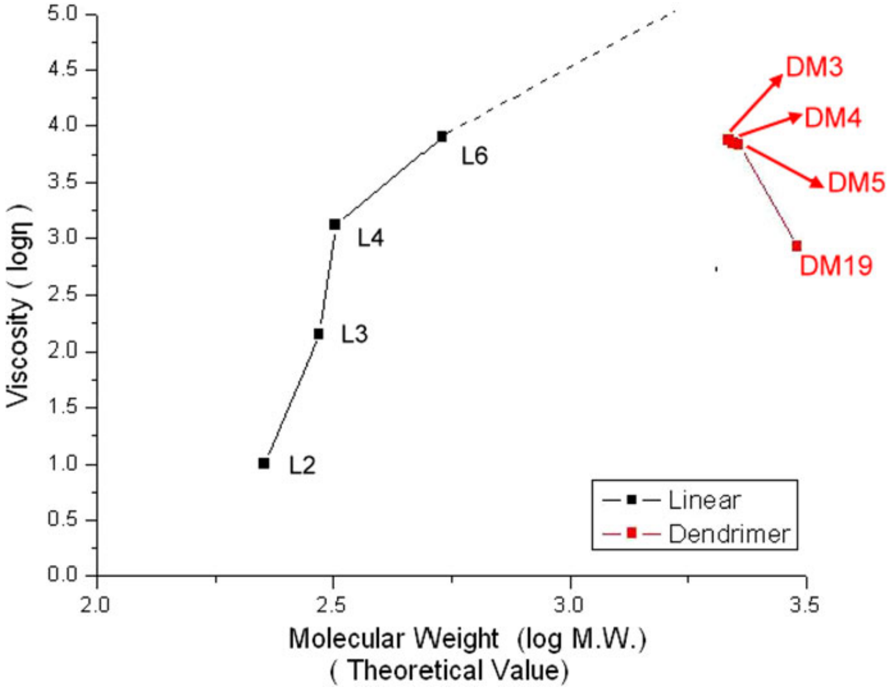

Fig. 3 Viscosity as a function of molecular weight for traditional and dendrimer monomers

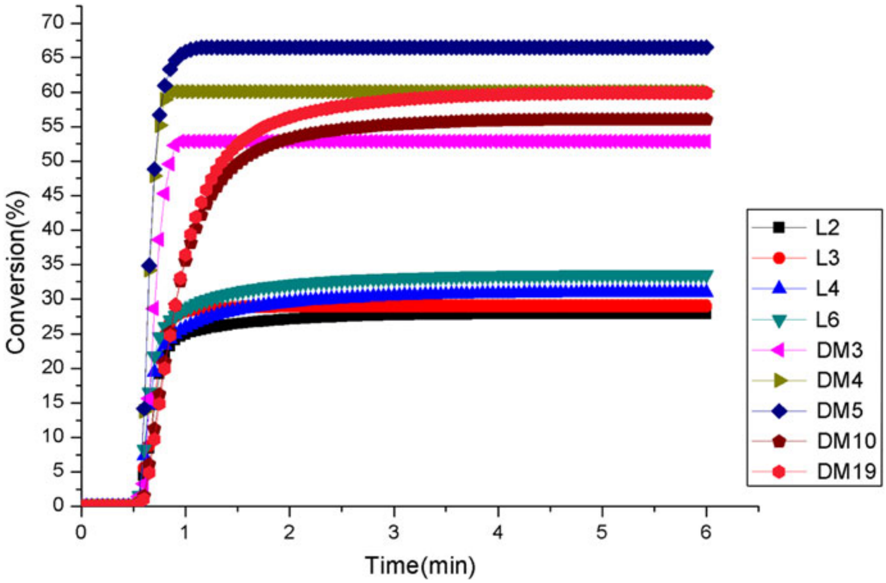

Fig. 4 Conversion ratio versus time through the treatment of original PDSC by Eq. 1 for traditional and dendrimer monomers

L-2. Finally, Fig. 4 demonstrates that the dendritic monomer with five acrylate sites has the highest conversion. For a dendrimer with ten or more branches, the final conversion ratios were then slightly lower at approximately 60%, and independent of the number of branches. All of the results shown above reveal that monomers attached with more acrylate groups have higher conversion ratio than others, because the double bond reaction within a dense group of multiacrylate sites is associated with a shorter period of free-radical propagation than a loose group of separate acrylate sites. Previous findings that the dendritic monomer has a better conversion ratio than the regular monomer and that L-6 has the highest conversion ratio of regular monomers confirm the above inference. However, the steric hindrance of the simultaneous occurrence of free-radical propagation dendrimers with multireactive branches would suppress the conversion ratio as the number of branches becomes extremely high, optimizing the conversion of dendrimer at a specific number of acrylate sites. In short, Fig. 4 indicates that the conversion ratio was maximal for dendrimer attached with five acrylate sites.

Figure 4 can be further converted to Fig. 5 which plots the derivative of the conversion ratio, representing the curing rate R_p, against the conversion ratio, $\boldsymbol{\alpha}$. Notably, the solid line in Fig. 5 is the result of curve fitting using the autocatalyzed reaction model (Eq. 3) [24, 25], which is often used for describing the reaction rate of UV curing.

$$\mathrm{d}\alpha/\mathrm{d}t = k\alpha^{m}(1-\alpha)^{n} \tag{3}$$

where m is the order of the autocatalyzed reaction, n is the order of the catalyzed reaction; k is the rate constant of the reactions, and α is the reaction conversion ratio

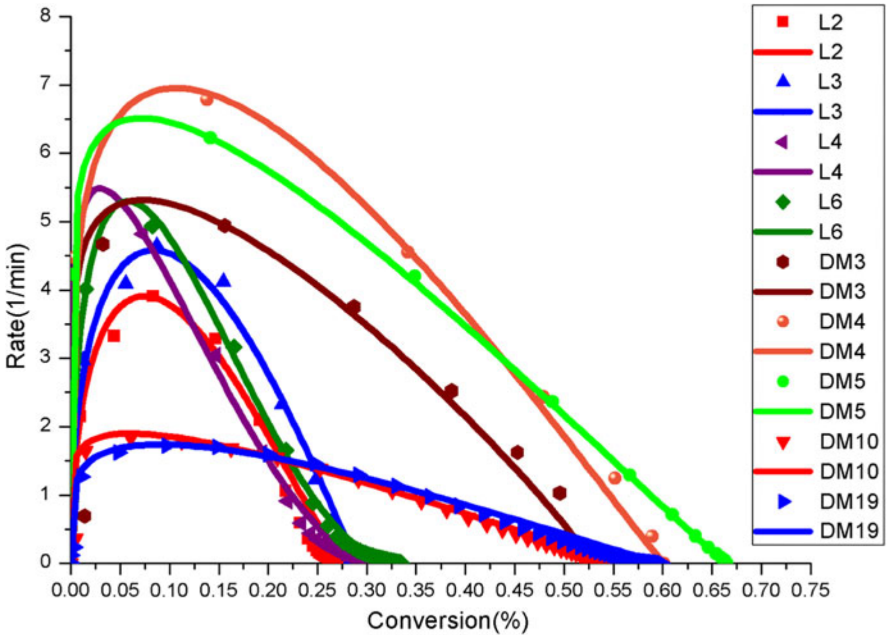

Fig. 5 Polymerization rate as a function of conversion ratio for traditional and dendrimer monomers

at a particular temperature. All traditional monomers reach the highest curing rate roughly at the same conversion ratio, approximately 10%. The dendritic monomers, however, have a very different rate over a broad range of conversion ratios. The curing rate of dendrimers, similar to the conversion ratio mentioned previously, initially increases with the number of acrylate sites, reaching the maximum at five branches. It is due to the fact that the free-radical initiation for the double bond in a dense group of multiacrylate sites is faster than that associated with regular monomer or dendrimer having few acrylated branches. Nevertheless, the curing rate in a dendrimer decreased as the acrylate sites increased further. The steric hindrance by the branches for the simultaneous free-radical propagation is believed to inhibit the curing process of dendrimers.

Table 2 tablets the measured and calculated results of curing kinetics based on Eq. 3. Dendrimers with higher acrylate sites such as DM10 and DM19 have lower rate constant k, even their final conversion is still high. Moreover, the autocatalyzed order m of a dendrimer is observed to be one half or even one-third as much of a regular monomer. This is attributed to the steric hindrance by the branches for the free-radical propagation as mentioned above.

Table 3 presents the hardness, and refractive index of cured films, made of either regular or dendritic monomers that contain various numbers of acrylate sites. Figure 6 presents the degradation temperature. The regular monomers have superior hardness and degradation temperature T_d to those of dendritic monomers. The heterogeneity of the cross-linking density of dendrimers is primarily responsible for their having lower hardness and lower T_d than the regular monomers. Cross-linking

Table 2 Measured and simulated results of UV curing by Eq. 3

	ΔH (J/g)	k	m	n	Conversion (α)
L2	212.587	10.539	0.457	1.251	27.9
L3	247.240	11.141	0.427	1.051	29
L4	299.083	10.144	0.1888	1.751	30.9
L6	295.984	16.537	0.4272	2.051	33.5
DM3	62.611	8.140	0.1468	0.914	52.9
DM4	92.488	12.642	0.2274	1.052	60.1
DM5	124.878	10.730	0.1268	1.051	66.5
DM10	199.883	2.844	0.1255	1.053	56.0
DM19	320.511	2.941	0.1870	1.100	60.0

Table 3 The hardness and refractive index of cured films, made of either regular or dendritic monomers containing various acrylate sites

	DM-3	DM-4	DM-5	DM-10	DM-19	L-4	L-6
Hardness	<B	HB	B	3H	6H	4H	6H
Refractive index	1.482	1.483	1.484	1.488	1.501	1.482	1.488

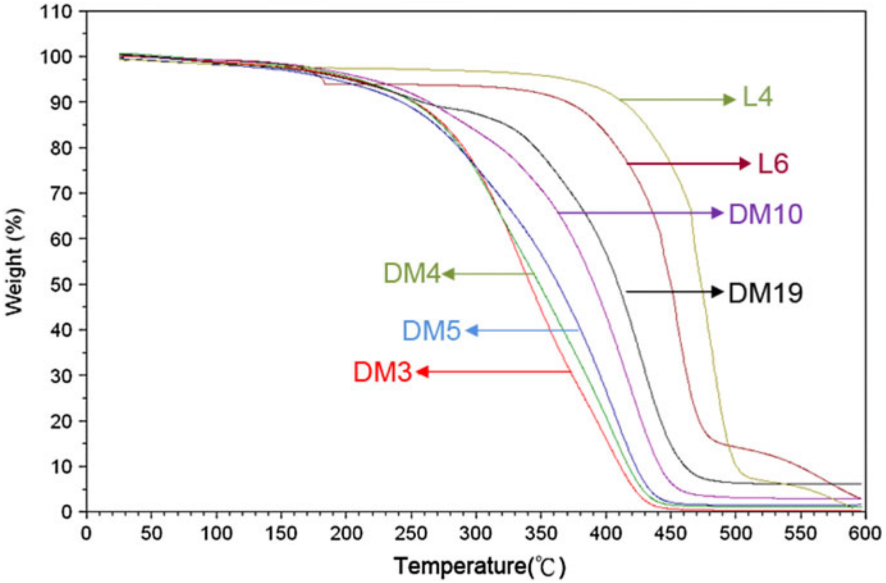

Fig. 6 TGA thermograms of dendrimer monomers and traditional monomers

points usually surround the dendrimer core at a given radius that depends on the generation number of the dendrimer. Restated, much space is occupied in the absence of a cross-linking point between the center and the edge of the dendrimer, causing inhomogeneity of cross-linking density. The regular monomers, however, form a film with a uniform crosslinking density, and outperform the others in terms of hardness and thermal degradation. Interestingly, a dendrimer with many acrylate sites, such as 19 (DM-19 of Table 3), can overcome the aforementioned disadvantages. DM-19 has very low viscosity, and thus avoids the traditional problem that a regular monomer with more than six branches makes coating impossible due to extremely high viscosity. Moreover, DM-19 has a refractive index of over 1.5, which is a typical target for films with optical applications. According to the Lorentz–Lorenz equation, the refractive index is proportional to (molar volume)$^{-1}$. DM-19 has the most compact structure, yielding the smallest molar volume to obtain the highest refractive index. In short, the inhomogeneity of the cross-linking density of dendrimers causes them to have lower hardness and lower T_d values than regular monomers. However, a dendrimer film with 19 acrylated branches can provide satisfactory hardness (6H), good T_d (290 °C) value, and a superior refractive index (1.5).

Conclusions

Experimental results show that even given the slightly higher MW of regular monomers, the viscosity increased rapidly with the number of branches. In contrast, a dendritic monomer with the same number of branches has a much lower viscosity. The conversion of hydroxyl groups into acrylic groups in the dendritic monomer slightly reduces the viscosity by eliminating the hydrogen bonds. Regarding to the effect of the number of acrylate sites on the curing reaction, the conversion ratio and curing rate initially increased, reaching the maximum at five branches. The acceleration of double bond reaction within a dense group of multiacrylate sites causes the initial rise, but the steric hindrance of simultaneous free-radical propagation by the branches slows down the reaction in dendrimer curing as the number of branches further increases. The autocatalyzed reaction model was then applied to analyze the curing kinetics. Dendrimers with 10–19 acrylate sites were found to have lower rate constant k and smaller autocatalyzed order m than the regular ones. Finally, the heterogeneity of the cross-linking density of dendrimers causes them to have weaker hardness and lower T_d values than the regular monomers. However, a dendrimer film with 19 acrylated branches provides satisfactory hardness (6H), good T_d (290 °C), and a high refractive index (1.5).

Acknowledgment The authors would like to thank the National Science Council of the Republic of China for financially supporting this research under Contract No. NSC-92-2622-E-027-009-CC3.

References

1. Fouassier JP (1995) Photoinitiation, photopolymerization, and photocuring: fundamentals and applications. Hanser Publishers, New York
2. Mezzenga R, Boogh L, Pettersson B, Manson JAE (2000) Effects of the branching architecture on the reactivity of epoxy-amine groups. Macromolecules 33(12):4373–4379

3. Anseth KS, Newman SM, Bowman CN (1995) Polymeric dental composites: properties and reaction behavior of multimethacrylate dental restorations. Adv Polym Sci 122:177–217
4. Anseth KS, Quick DJ (2001) Polymerizations of multifunctional anhydride monomers to form highly crosslinked degradable networks. Macromol Rapid Commun 22(8):564–572
5. Decker C, Moussa K (1990) UV-radiation and laser-induced polymerization of acrylic monomers. ACS Symp Ser 417:439–456
6. Decker C (1992) Kinetic study of light-induced polymerization by real-time UV and IR spectroscopy. J Polym Sci A Polym Chem 30(5):913–928
7. Mailhot G, Bolte M (1991) Bimetallic systems for acrylamide photosensitized polymerization Part II. Cr^{VI} Cu^{II}, a suitable system to control the polymerization process. J Photochem Photobiol A 56(2–3): 387–396
8. Paczkowski J, Neckers DC (1991) Twisted intramolecular charge-transfer phenomenon as a quantitative probe of polymerization kinetics. Macromolecules 24(10):3013–3016
9. Song JC, Neckers DC (1996) Characterization of photocurable coatings using fluorescence probes. Polym Eng Sci 36(3):394–402
10. Small RD, Ors JA, Royce BSH (1984) Photopolymer dielectrics: the characterization of curing behavior for modified acrylate systems. HYPERLINK “http://pubs.acs.org/isbn/9780841208230” “View Table of Contents”. ACS Symp Ser 242:325–344
11. Watanabe K, Amari T, Otsubo V (1984) Dynamic viscoelastic measurements of photosensitive polymers. J Appl Polym Sci 29(1):57–66
12. Nelson EW, Jacobs JL, Scranton AB, Anseth KS, Bowman CN (1995) Photo-differential scanning calorimetry studies of cationic polymerizations of divinyl ethers. Polymer 36(24):4651–4656
13. Bunyan PF, Cunliffe AV (1996) Microcalorimetric determination of the cure reaction in some fluorinated polyether rubbers. Thermochim Acta 276:131–144
14. Lecamp L, Youssef B, Bunel C, Lebaudy P (1997) Photoinitiated polymerization of a dimethacrylate oligomer: 1. Influence of photoinitiator concentration, temperature and light intensity. Polymer 38(25):6089–6096
15. Scott TF, Cook WD, Forsythe JS (2002) Photo-DSC cure kinetics of vinyl ester resins. I. Influence of temperature. Polymer 43(22):5839–5845
16. Asif A, Huang CY, Shi WF (2003) UV curing behaviors and hydrophilic characteristics of UV curable waterborne hyperbranched aliphatic polyesters. Polym Adv Technol 14(9):609–615
17. Xu G, Zhao YB, Shi WF (2005) Properties and morphologies of UV-cured epoxy acrylate blend films containing hyperbranched polyurethane acrylate/hyperbranched polyester. J Polym Sci B Polym Phys 43(22):3159–3170
18. Si QF, Wang X, Fan XD, Wang SJ (2005) Synthesis and characterization of ultraviolet-curable hyperbranched poly(siloxysilane)s. J Polym Sci Polym Chem 43(9):1883–1894
19. Schmidt LE, Leterrier Y, Schamh D, Manson JA, James D, Gustavsson E, Svensson L (2007) Conversion analysis of acrylated hyperbranched polymers UV-cured below their ultimate glass transition temperature. J Appl Polym Sci 104(4):2366–2376
20. Asif A, Shi WF (2004) UV curable waterborne polyurethane acrylate dispersions based on hyperbranched aliphatic polyester: effect of molecular structure on physical and thermal properties. Polym Adv Technol 15(11):669–675
21. Wang SJ, Fan XD, Kong J, Liu YY (2008) Synthesis, characterization, and UV curing kinetics of hyperbranched polycarbosilane. J Appl Polym Sci 107(6):3812–3822
22. Guymon CA, Bowman CN (1997) Polymerization behavior and kinetics during the formation of polymer-stabilized ferroelectric liquid crystals. Macromolecules 30(6):1594–1600
23. Avci D, Nobles J, Mathias LJ (2003) Synthesis and photopolymerization kinetics of new flexible diacrylate and dimethacrylate crosslinkers based on C18 diacid. Polymer 44(4):963–968
24. Cho JD, Ju HT, Hong JW (2005) Photocuring kinetics of UV-initiated free-radical photopolymerizations with and without silica nanoparticles. J Polym Sci Polym Chem 43(3):658–670
25. Boey F, Rath SK, Ng AK, Abadie MJM (2002) Cationic UV cure kinetics for multifunctional epoxies. J Appl Polym Sci 86(2):518–525